Multi-component optical azimuthons of four-wave mixing*

Wang Rui-Min(王瑞敏), Wang Xing-Peng(王兴鹏), Wu Zhen-Kun(吴振坤), Yao Xin(姚 鑫), Zhang Yi-Qi(张贻齐), and Zhang Yan-Peng(张彦鹏)†

School of Science & Key Laboratory for Physical Electronics and Devices of the Ministry of Education & Shaanxi Key Lab of Information Photonic Technique, Xi'an Jiaotong University, Xi'an 710049, *China*

(Received 22 September 2013; revised manuscript received 15 November 2013; published online 25 March 2014)

We report the multi-component optical azimuthons of four-wave mixing (FWM) composed of several modulated vortex beams, the so-called azimuthons, in V-type three-level and two-level atomic systems. We analyze the formation mechanisms of the FWM azimuthons theoretically and experimentally. In addition, we illustrate the interactions between the co-propagating azimuthon components. Finally, we also compare the stabilities of azimuthons in V-type three-level and two-level atomic systems.

Keywords: nonlinear optics, four-wave mixing, Kerr effect

PACS: 42.65.–k, 42.65.Tg, 42.65.Jx **DOI:** 10.1088/1674-1056/23/5/054209

1. Introduction

Optical vortexes are self-trapped localized beams with spiral phase structures and phase singularities. In the last two decades, optical vortexes have attracted a lot of attention and a large amount of literature on this topic has been published. Among the various progress reports, the ring-shaped vortex solitons are quite involved.[1] It was shown that such solitons undergo an azimuthal instability in self-focusing medium. Another well-known example of the self-trapped vortex beams are the soliton clusters, which can merge into fundamental or vortex solitons, based on the model of laser cavities.[2] Several years ago, a novel self-trapped localized vortex beam, named azimuthon, was reported.[3] Such spatially modulated vortex beams provide a link between ring-shaped vortex and soliton clusters. It is worth mentioning that the optical vortex solitons are not only reported in bulk media, but also researched in waveguides,[4] Bose–Einstein condensates,[5] atomic vapors,[6–11] quantum dots,[12] discrete systems,[13] and so on. Recently, we have observed modulated vortex solitons of four-wave mixing (FWM) in multi-level atomic systems that are governed by cross-phase modulation (XPM).[6–9] The XPM can enhance the transmission stability of spatial solitons.[14]

When two or more field components propagate together, the interaction between the components results in vector solitons. It is demonstrated that a strong fundamental component traps a ring-shaped vortex (or necklace-shaped) soliton that can form vortex[15] (or multipole) vector solitons.[16] At the same time, the ring vortex waveguide induced by a strong vortex component also supports double-vortex vector solitons.[17] However, as far as we are aware, there have been few previous reports of vector azimuthons. Multiple four-wave-mixing processes are effective methods to obtain vector azimuthons. They have also been used to produce multifrequency lasers, which have important applications in optical fiber communication.[18,19]

In this work, we first investigate the scalar and vector optical azimuthons of FWM in V-type three-level and two-level atomic systems. The effect of the XPM on the formation of the scalar FWM azimuthons is discussed. The interaction of the multi-component azimuthons is analyzed. In addition, the stabilities of azimuthons in V-type three-level and two-level atomic systems are also compared. These investigations not only enrich the understanding on optical azimuthons, but also have potential applications in future all-optical manipulations.

2. Experiments

The experiments are carried out in two different energy-level configurations in Na atom vapors (the atomic vapor is heated with an atomic density of 5.6×10^{13} cm^{-3}): V-type three-level and two-level systems. As shown in Fig. 1(a), energy levels $|0\rangle$ $(3S_{1/2})$, $|1\rangle$ $(3P_{1/2})$, and $|2\rangle$ $(3P_{3/2})$ form a complex V-type atomic system by employing six laser beams. When six laser beams are all modulated to connect the transition $|0\rangle \rightarrow |2\rangle$, the atomic system changes into a two-level system, as shown in Fig. 1(b). The spatial alignment of the beams is displayed in Fig. 1(c). Two pump beams (E_1 and E_2) propagate in the same direction, and two probe beams (E_3 and E_3') propagate in the opposite direction of E_1 and E_2. The dressing

*Project supported by the National Basic Research Program of China (Grant No. 2012CB921804), the National Natural Science Foundation of China (Grant Nos. 61308015, 11104214, 61108017, 11104216, and 61205112), the Specialized Research Fund for the Doctoral Program of Higher Education of China (Grant Nos. 20110201110006 and 20110201120005), the Fundamental Research Funds for the Central Universities of Ministry of Education of China (Grant Nos. 2012jdhz05, 2011jdhz07, xjj2011083, xjj2011084, xjj2012080, and xjj2013089), and China Postdoctoral Science Foundation (Grant No. 2012M521773).

†Corresponding author. E-mail: ypzhang@mail.xjtu.edu.cn

© 2014 Chinese Physical Society and IOP Publishing Ltd

beam E_1' (E_2') propagates with angle $\theta_1 \approx 0.3^\circ$ ($\theta_2 \approx 0.3^\circ$) between $E_1(E_2)$. Three laser beams E_1 (with frequency ω_1, wavevector $\boldsymbol{k}_1$, and Rabi frequency G_1), E_1' (ω_1, $\boldsymbol{k}_1'$, G_1') and E_3 (ω_1, $\boldsymbol{k}_3$, G_3) come from the same dye laser DL1 (10-Hz repetition rate, 5-ns pulse width, and 0.04-cm^{-1} linewidth)

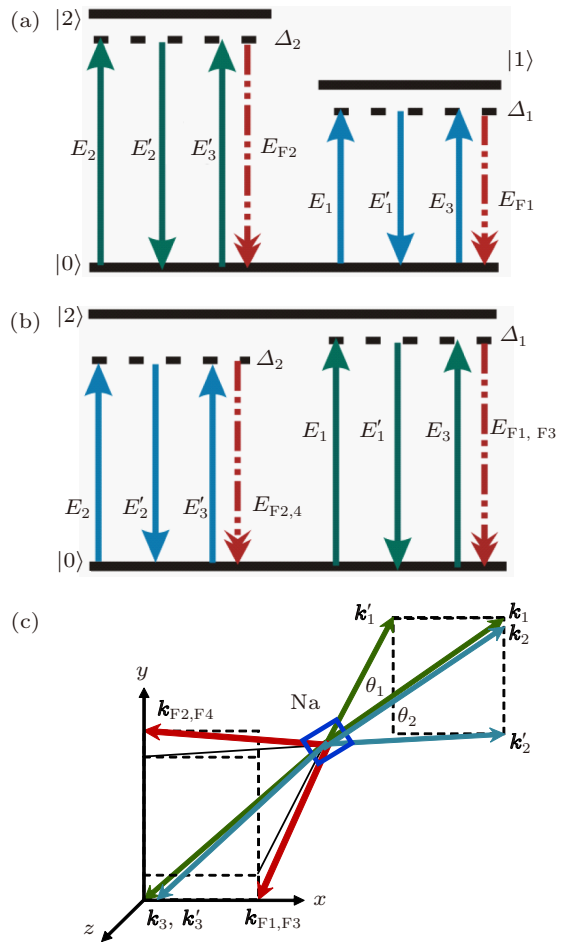


Fig. 1. (a) V-type three-level and (b) Two-level atomic systems with six laser beams. (c) Spatialbeam geometry used in the experiment.

with the frequency detuning $\Delta_1 = \Omega - \omega_1$, where Ω is the resonant frequency. The other three laser beams E_2 (ω_2, $\boldsymbol{k}_2$, G_2), E_2' (ω_2, $\boldsymbol{k}_2'$, G_2'), and E_3' (ω_2, $\boldsymbol{k}_3'$, G_3') are from another dye laser DL2 (which has the same characteristics as the DL1) with a frequency detuning $\Delta_2 = \Omega - \omega_2$. In a V-type three-level system, two degenerate-FWM (DFWM) signals $E_{\rm F1}$ (with phase-matching condition $\boldsymbol{k}_{\rm F1} = \boldsymbol{k}_1 - \boldsymbol{k}_1' + \boldsymbol{k}_3$), $E_{\rm F2}$ ($\boldsymbol{k}_{\rm F2} = \boldsymbol{k}_2 - \boldsymbol{k}_2' + \boldsymbol{k}_3'$) and two non-DFWM (NDFWM) signals $E_{\rm F3}$ ($\boldsymbol{k}_{\rm F3} = \boldsymbol{k}_1 - \boldsymbol{k}_1' + \boldsymbol{k}_3'$), $E_{\rm F4}$ ($\boldsymbol{k}_{\rm F4} = \boldsymbol{k}_2 - \boldsymbol{k}_2' + \boldsymbol{k}_3$) are generated when all six laser beams are turned on. These generated FWM signals propagate in two directions (i.e., propagate in the opposite direction of $\boldsymbol{k}_1'$ and $\boldsymbol{k}_2'$, respectively). In the two-level atomic system, six laser beams have nearly degenerate frequencies. The interference between arbitrary pump beam and dressing beam can induce electromagnetic induced grating (EIG). The FWM signals can be considered to be a result of the electromagnetically-induced diffraction of the probe beam $\boldsymbol{E}_3$ or $\boldsymbol{E}_3'$ by EIG. Therefore, besides the four FWM signals mentioned above, there exist another four FWM signals: $E_{\rm F5}$ ($\boldsymbol{k}_{\rm F5} = \boldsymbol{k}_2 - \boldsymbol{k}_1' + \boldsymbol{k}_3$), $E_{\rm F6}$ ($\boldsymbol{k}_{\rm F6} = \boldsymbol{k}_2 - \boldsymbol{k}_1' + \boldsymbol{k}_3'$), $E_{\rm F7}$ ($\boldsymbol{k}_{\rm F7} = \boldsymbol{k}_1 - \boldsymbol{k}_2' + \boldsymbol{k}_3$), and $E_{\rm F8}$ ($\boldsymbol{k}_{\rm F8} = \boldsymbol{k}_1 - \boldsymbol{k}_2' + \boldsymbol{k}_3'$).

3. Optical azimuthons of four-wave mixing

First, we investigate the formation of the scalar azimuthons of FWM. The controllable optical vortex can be generated by the interference of three plane waves.[20] In the experiment of FWM, three laser beams E_1, E_1', and E_3 overlap in the medium, the destructive interference result in phase singularity at the position where the summed complex amplitude is zero. The summed complex amplitude of the interfered beams can be expressed as follows:

$$E = A_x \cos(\varphi + \delta_1) + \mathrm{i} A_y \cos(\varphi + \delta_2), \tag{1}$$

where

$$\delta_1 = -\arctan \frac{E_1 n_1 k_{1y} \sin T_{\psi 1} + E_1' n_{1'} k_{1'y} \sin T_{\psi 1'} + E_3 n_3 k_{3y} \sin T_{\psi 3}}{E_1 n_1 k_{1x} \sin T_{\psi 1} + E_1' n_{1'} k_{1'x} \sin T_{\psi 1'} + E_3 n_3 k_{3x} \sin T_{\psi 3}},$$

$$\delta_2 = -\arctan \frac{E_1 n_1 k_{1y} \cos T_{\psi 1} + E_1' n_{1'} k_{1'y} \cos T_{\psi 1'} + E_3 n_3 k_{3y} \cos T_{\psi 3}}{E_1 n_1 k_{1x} \cos T_{\psi 1} + E_1' n_{1'} k_{1'x} \cos T_{\psi 1'} + E_3 n_3 k_{3x} \cos T_{\psi 3}},$$

are the initial phases; $T_{\psi 1} = \psi_{10} + n_1(k_{1x}T_x + k_{1y}T_y)$, $T_{\psi 1'} = \psi_{1'0} + n_{1'}(k_{1'x}T_x + k_{1'y}T_y)$, and $T_{\psi 3} = \psi_{30} + n_3(k_{3x}T_x + k_{3y}T_y)$, with ($T_x$, T_y) being the coordinate of the singularity point; $n_1 = n_0 + n_2^{\rm X2}|E_1'|^2 + n_2^{\rm X5}|E_3|^2$, $n_{1'} = n_0 + n_2^{\rm X1}|E_1|^2 + n_2^{\rm X5}|E_3|^2$, and $n_3 = n_0 + n_2^{\rm X1}|E_1|^2 + n_2^{\rm X2}|E_1'|^2$ are the nonlinear refractive indexes with $n_2^{\rm X} = {\rm Re}\chi^{(3)}/(\varepsilon_0 c n_1)$ being the cross-Kerr nonlinear coefficient. Typically, the electrical field of the vortex beam can be written as $E(r,\varphi,z) = U(r)\exp[\mathrm{i}\Phi(r,\varphi,z)]$, where $\Phi(r,\varphi,z) = kr^2/2R(z) + m\varphi + kz$ is the phase and R is the radius of the wave front curvature. Comparing Eq. (1) with the azimuthal phase, it can be deduced that the topological charge carried by the FWM vortex is $m = 1$ or $m = -1$. The direction of rotation is controlled by the initial phases of interfered lights. When $0 < \delta_2 - \delta_1 < \pi$ ($\pi < \delta_2 - \delta_1 < 2\pi$), $m = 1$ ($m = -1$), the vortex rotates clockwise (anticlockwise).

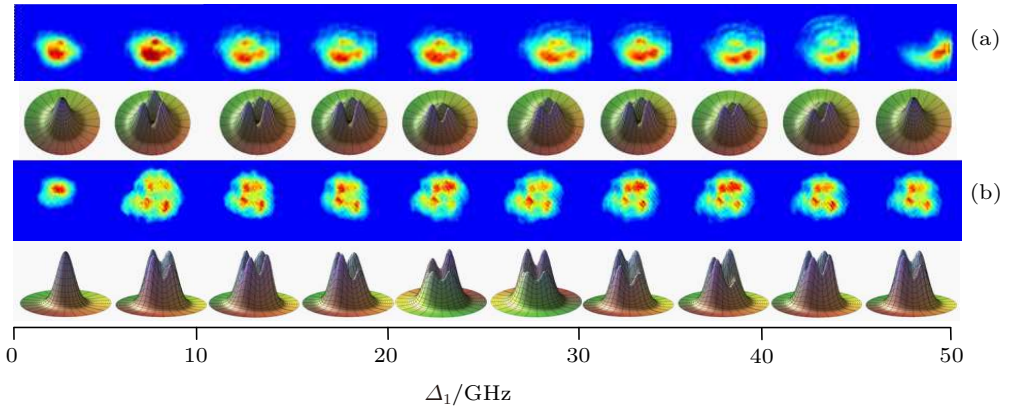


Fig. 2. Azimuthons formed from probe beam E_3 with (a) one dressing field E_1' and (b) two dressing fields E_1' and E_2'. Upper and lower panels in (a) and (b) are for experimental and simulated results, respectively.

In a self-defocusing nonlinear medium, a beam with phase singularity may get self-trapped and generate a vortex soliton. In contrast, vortex solitons become unstable in the self-focusing region.[8] Figure 2 shows the azimuthons of the probe beam E_3 in the self-defocusing region. In our experiment, the dressing beams $E_{1,2}'$ are approximately 1000 times stronger than the weak probe beam E_3, E_3' and the generated FWM beams. Such strong dressing fields co-propagate with the probe beams and FWM signals in nonlinear medium, the XPM can strongly affect the azimuthal intensity and phase of the FWM vortex, which leads to the formation of azimuthons. As Fig. 2(a) shows, with one dressing field E_1' on, E_3 splits into three spots along a ring. When two dressing fields E_1' and E_2' are on (Fig. 2(b)), E_3 splits into four spots. At resonance $\Delta_1 = 0$ and the large detuning points, E_3 fuse into a fundamental spot. These phenomena are ascribed to the cross-Kerr nonlinear dispersion induced by the dressing fields. As a result, the phase of the vortex beam will change. The nonlinear phase shift induced by the dressing field at a position of vortex beam can be written as

$$\phi_n = \frac{2kn_2^{\mathrm{X}}I'}{n_0 I_0}\,\mathrm{e}^{-[r^2+r_0^2-2rr_0\cos(\varphi-\varphi_0)]/w^2}z, \tag{2}$$

where r_0 and φ_0 are the relative distance and angle of the dressing field to phase singularity of the vortex, respectively; I' and I_0 are the intensities of the dressing field inducing Kerr nonlinearity and the vortex beam, respectively, $n_2^{\mathrm{X}} = \mathrm{Re}\chi^{(3)}/(\varepsilon_0 c n_1)$ is the cross-Kerr coefficient and $\chi^{(3)}$ is the third-order nonlinear susceptibility. The additional transverse wave vector introduced by the cross-Kerr nonlinearity is

$$\begin{aligned}\delta\boldsymbol{k}_\perp &= \delta\boldsymbol{k}_r + \delta\boldsymbol{k}_\varphi \\ &= -\frac{4kn_2^{\mathrm{X}}I'z}{n_0 I_0 w^2}\,\mathrm{e}^{-[r^2+r_0^2-2rr_0\cos(\varphi-\varphi_0)]/w^2} \\ &\quad\times\{[r-r_0\cos(\varphi-\varphi_0)]\hat{\boldsymbol{r}} + r_0\sin(\varphi-\varphi_0)\hat{\boldsymbol{\varphi}}\}. \end{aligned}\tag{3}$$

This anisotropic transverse wave vector induces azimuthal intensity and phase modulation into a vortex beam, which can change the rotation rate of vortex and globally split the vortex beam. Therefore, the cross-phase modulated azimuthon forms. The electrical field of such azimuthons can be written as

$$\begin{aligned}E(r,\varphi,z) &= E_0\tanh\Big(\frac{r}{w_v}\Big)\exp\Big(-\frac{r^2}{w(z)^2}\Big) \\ &\quad\times\Big[\cos\Big(\frac{N\varphi}{2}\Big)+\mathrm{i}p\sin\Big(\frac{N\varphi}{2}\Big)\Big] \\ &\quad\times\exp\big[\mathrm{i}\Phi(r,\varphi,z)+\mathrm{i}\phi_n(r,\varphi,z)\big], \end{aligned}\tag{4}$$

in which p is the modulation parameter ($1-p$ is the modulation depth), and N is the number of intensity peaks. Such cross-Kerr nonlinear modulated azimuthon has three different factors: the topological charge m, the number of intensity peaks N, and the modulation depth $1-p$. The angular momentum of such an azimuthon is $M_a = \int (m + r\delta\boldsymbol{k}_\varphi)U^2(r)\,\mathrm{d}r$. When two dressing fields E_1' and E_2' are both on, the nonlinear phase shift is induced by two dressing fields simultaneously. In this case

$$\begin{aligned}\phi_n &= \frac{2kn_2^{\mathrm{X}}I_1'}{n_0 I_0}\,\mathrm{e}^{-[r^2+r_1^2-2rr_1\cos(\varphi-\varphi_1)]/w^2}z \\ &\quad+\frac{2kn_2^{\mathrm{X}}I_2'}{n_0 I_0}\,\mathrm{e}^{-[r^2+r_2^2-2rr_2\cos(\varphi-\varphi_2)]/w^2}z. \end{aligned}\tag{5}$$

Therefore, the probe field E_3 further splits into four spots. At resonance ($\Delta_1 = 0$) and large frequency detuning, they decay into a fundamental spot because the nonlinear refractive index n_2^{X} and the nonlinear phase shift ϕ_n are close to zero.

Figure 3(a) gives the FWM signals E_{F1} and E_{F3} in V-type three-level system. When three laser beams E_1, E_1', E_3 and the dressing field E_2' are turned on, the DFWM signal E_{F1} is generated and dressed by E_2'. The dressed perturbation chain of E_{F1} is written as: $\rho_{00}^{(0)} \xrightarrow{E_1} \rho_{1G_2\pm}^{(1)} \xrightarrow{(E_1')^*} \rho_{G_2\pm 0}^{(2)} \xrightarrow{E_3} \rho_{1G_2\pm}^{(3)}$. Here, the expression of the corresponding density matrix of FWM signal E_{F1} is

$$\rho_{\mathrm{F1}}^{(3)} = \frac{-\mathrm{i}G_3G_1(G_1')^*}{\Big(\Gamma_{00}+\dfrac{G_2^2}{\mathrm{i}\Delta_2+\Gamma_{20}}\Big)\Big[\mathrm{i}\Delta_1+\Gamma_{10}+\dfrac{G_2^2}{\Gamma_{12}+\mathrm{i}(\Delta_2+\Delta_1)}\Big]^2}. \tag{6}$$

Therefore, the third-order nonlinear susceptibility is $\chi^{(3)} = D\rho_{\rm F1}^{(3)}$, where $D = n\mu_{10}^4/(\hbar^3\varepsilon_0 G_{\rm F1}G_1^2)$ ($G_{\rm F1}$ is the Rabi frequency of $E_{\rm F1}$), n is the atomic density and μ_{10} is the dipole-matrix element between energy levels $|0\rangle$ and $|1\rangle$. From Eq. (6), we can get the nonlinear phase shift $\phi_{\rm F1}$ at different frequency detuning. It can be seen in Fig. 3(a), at small frequency detuning Δ_1 in self-defocusing region, the DFWM signal $E_{\rm F1}$ forms a three-spot azimuthon. With the increase of Δ_1, $E_{\rm F1}$ decays into a tilted dipole-type beam. The tilt of the dipole beam indicates the spatial twist in beam $E_{\rm F1}$. Such a dipole azimuthon is due to the initial angular momentum of the vortex beam transferred to the orbital angular momentum of dipole splinters. The conservation of angular momentum is satisfied in this interaction process.

When four laser beams E_1, E_1', E_2', and E_3' are turned on, the NDFWM signal $E_{\rm F3}$ is generated through $\rho_{00}^{(0)} \xrightarrow{E_1} \rho_{1G_2\pm}^{(1)} \xrightarrow{(E_1')^*} \rho_{G_2\pm 0}^{(2)} \xrightarrow{E_3'} \rho_{20}^{(3)}$ and dressed by E_2'. For $E_{\rm F3}$, the expression of the density matrix is

$$\rho_{\rm F3}^{(3)} = \frac{-{\rm i}G_3'G_1(G_1')^*}{\left(\Gamma_{00}+\dfrac{G_2^2}{{\rm i}\Delta_2+\Gamma_{20}}\right)\left[{\rm i}\Delta_1+\Gamma_{10}+\dfrac{G_2^2}{{\rm i}(\Delta_1-\Delta_2)+\Gamma_{12}}\right]({\rm i}\Delta_2+\Gamma_{20})}. \quad (7)$$

In the self-defocusing region, the NDFWM signal $E_{\rm F3}$ shows the horizontal dipole shape. We cannot get the vortex of the NDFWM signal because of the larger frequency difference among three generating fields E_1, E_1', and E_3' in V-type three-level, which prevent the interference from forming a phase singularity. The dipole pattern of $E_{\rm F3}$ results from the horizontal electromagnetic induced grating induced by E_1 and E_1'.[8]

Figure 3(b) shows four FWM signals $E_{\rm F1}$, $E_{\rm F3}$, $E_{\rm F5}$, and $E_{\rm F6}$ dressed by E_2' in a two-level atomic system. The density matrices for four FWM processes are

$$\rho_{\rm F1}^{(3)} = \frac{-{\rm i}G_3G_1(G_1')^*}{\left(\Gamma_{00}+\dfrac{G_2^2}{{\rm i}\Delta_2+\Gamma_{20}}\right)\left[{\rm i}\Delta_1+\Gamma_{20}+\dfrac{G_2^2}{\Gamma_{00}+{\rm i}(\Delta_1-\Delta_2)}\right]^2}, \quad (8)$$

$$\rho_{\rm F3}^{(3)} = \frac{-{\rm i}G_3'G_1(G_1')^*}{\left(\Gamma_{00}+\dfrac{G_2^2}{{\rm i}\Delta_2+\Gamma_{20}}\right)\left[{\rm i}\Delta_1+\Gamma_{20}+\dfrac{G_2^2}{{\rm i}(\Delta_1-\Delta_2)+\Gamma_{00}}\right]({\rm i}\Delta_2+\Gamma_{20})}, \quad (9)$$

$$\rho_{\rm F5}^{(3)} = \frac{-{\rm i}G_3G_2(G_1')^*}{\left(\Gamma_{20}+{\rm i}\Delta_2+\dfrac{G_2^2}{\Gamma_{00}}\right)^2\left[\Gamma_{00}+{\rm i}(\Delta_2-\Delta_1)+\dfrac{G_2^2}{\Gamma_{20}+{\rm i}(2\Delta_2-\Delta_1)}\right]}, \quad (10)$$

$$\rho_{\rm F6}^{(3)} = \frac{-{\rm i}G_3'G_2(G_1')^*}{\left(\Gamma_{20}+{\rm i}\Delta_2+\dfrac{G_2^2}{\Gamma_{00}}\right)\left[\Gamma_{00}+{\rm i}(\Delta_2-\Delta_1)+\dfrac{G_2^2}{\Gamma_{20}+{\rm i}(2\Delta_2-\Delta_1)}\right][\Gamma_{20}+{\rm i}(2\Delta_2-\Delta_1)]}. \quad (11)$$

In a two-level system, six laser beams ($E_{1,2,3}$ and $E_{1,2,3}'$) have nearly degenerate frequency. Therefore, besides the degenerated FWM signal $E_{\rm F1}$, the three generating fields of arbitrary non-degenerated FWM signals can also interfere to form phase singularity. It can be observed three-spot azimuthons of both DFWM and NDFWM signals in the self-defocusing region. At resonance and large frequency detuning, they also decay into fundamental spots because of the decrease of ϕ_n. In these processes, the conservation of the topological charges must be fulfilled. The topological charges of the FWM signals are determined by $m_{\rm F1} = m_1 - m_1' + m_3$, $m_{\rm F3} = m_1 - m_1' + m_3'$, $m_{\rm F5} = m_2 - m_1' + m_3$, and $m_{\rm F6} = m_2 - m_1' + m_3'$, where $m_{1,2,3}$ and $m_{1,2,3}'$ are the topological charges of $E_{1,2,3}$ and $E_{1,2,3}'$, respectively.

The modulation parameter p is an important factor that is used to describe azimuthons. With the value of p changing continuously from $p = 0$ to $p = 1$, the corresponding beam transforms from multipole structure to azimuthons and then vortex. The phase also transforms from the step phase to the spiral phase structure. On the other hand, the rotation angular velocity of azimuthons changes with different values of p. The spin of azimuthons is given by $S = 2mp/(1+p^2)$.[15] Now, we discuss the controlling of the modulation parameter p of azimuthons in FWM process. It is known that the splitting of the FWM vortex results from the XPM of the dressing fields. As $\phi_n \propto I'/I_0$, the modulation parameter p can be controlled by the intensity of the dressing field I'.

Figure 4(a) shows the images of $E_{\rm F1}$ at different powers of dressing field E_2' in two-level system. When the dressing field is weak, ϕ_n and its splitting function are small, so the modulation depth $1-p \to 0$, which leads to a ring-like vortex. With the power of the dressing field E_2' increases, ϕ_n becomes greater. Accordingly, the modulation depth becomes deep, so the image of $E_{\rm F1}$ changes to three-spot azimuthons and finally forms a necklace-like beam. However, with a further increase of E_2' power, the FWM beam will be repulsed by E_2', so that $E_{\rm F1}$ moves away from the central position of the phase singularity mask that is generated by the interference of three laser beams E_1, E_1', and E_3. Therefore, the azimuthon structure of $E_{\rm F1}$ is substituted by a split strip pattern.

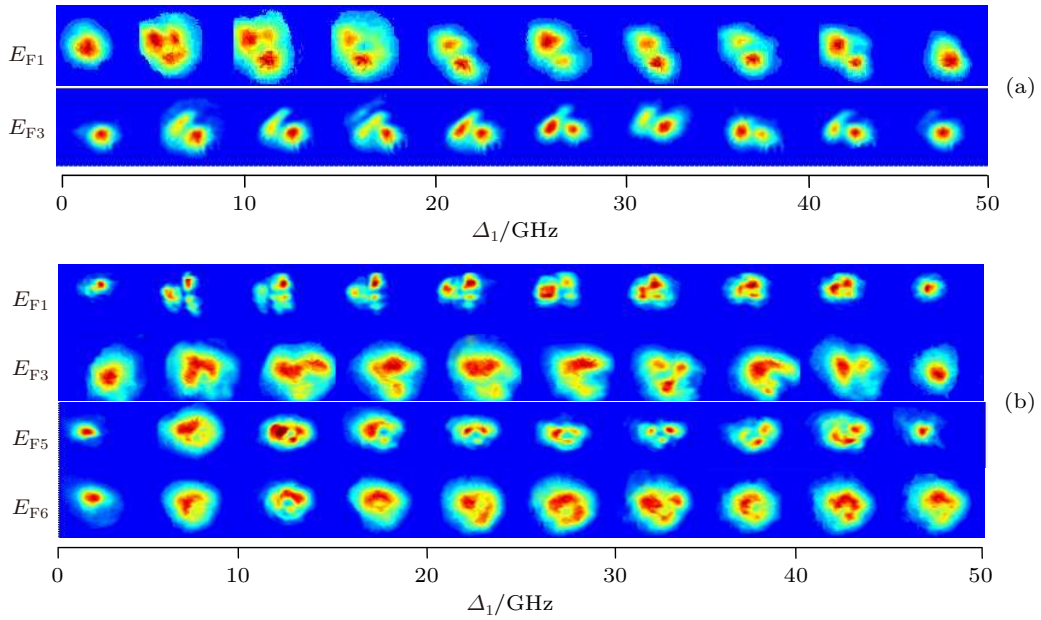


Fig. 3. (a) The FWM signals E_{F1} and E_{F3} in V-type three-level system dressed by E_2'. (b) The FWM signals E_{F1}, E_{F3}, E_{F5}, and E_{F6} in two-level atomic system dressed by E_2'.

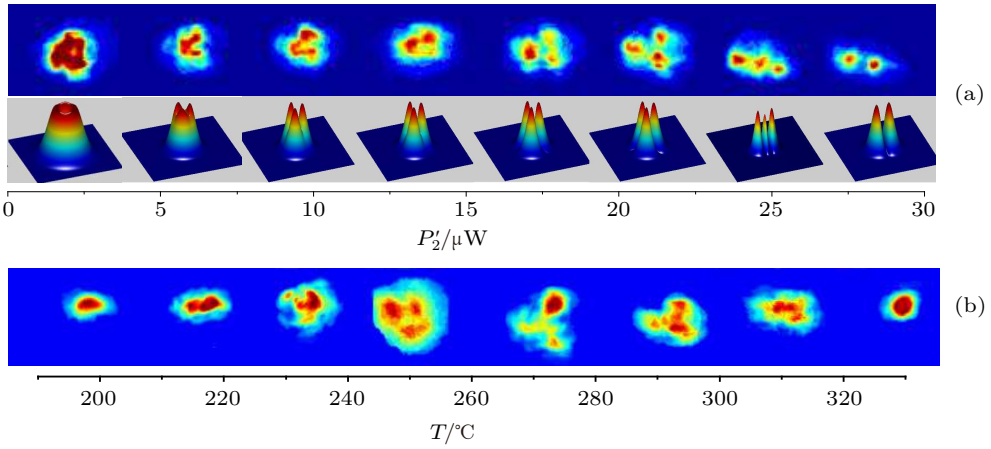


Fig. 4. (a) Images of E_{F1} versus the power of the dressing field E_2' in two-level system. The bottom row gives the numerical simulated results. (b) The temperature dependence of FWM signal E_{F1} in V-type three-level system.

Temperature is another factor that affects the evolution of spatial solitons.[21] Figure 4(b) describes the temperature dependence of FWM signal E_{F1} in V-type three-level system. As the temperature increases from 200 °C to 300 °C, the images of E_{F1} evolve from a single spot to azimuthon pattern. However, when the temperature is over 300 °C, E_{F1} again decays into a single spot. As discussed above, the third-order nonlinear susceptibility $\chi^{(3)} = n\mu_{10}^4\rho_{F1}^{(3)}/(\hbar^3\varepsilon_0 G_{F1}G_1^2)$ is proportional to the atomic density n. As the temperature increases, the atomic density n increases accordingly, which enlarges $\chi^{(3)}$ and ϕ_n. As a result, the FWM azimuthons form. However, the increase of temperature also causes greater absorption, which results in the decrease of beam intensity and, therefore, leads to smaller ϕ_n. Therefore, E_{F1} decays into a single spot at very high temperature. From our experiment, we find that the ideal temperature for the formation of FWM azimuthons is around 260 °C. In this case, the atomic density is about 5.6×10^{13} cm^{-3}, and the refractive index contrast is $\Delta n = n_2 I = 4.85\times10^{-4}$, approximately.

4. Multi-component optical azimuthons

In a nonlinear medium, the nonlinear coupling among several co-propagating azimuthon beams can form multi-component optical azimuthons. Figure 5(a) shows the two-component azimuthons observed in V-type three-level system in a self-defocusing nonlinear medium. In the experiment, four laser beams E_1, E_1', E_3, and E_3' are turned on. For two co-propagating probe beams E_3 and E_3', which are dressed by E_1', the incoherently coupled nonlinear Schrödinger equations can be written as

$$\frac{\partial E_3}{\partial z} - \frac{\mathrm{i}}{2k}\left(\frac{1}{r}\frac{\partial E_3}{\partial r} + \frac{\partial^2 E_3}{\partial r^2} + \frac{1}{r^2}\frac{\partial^2 E_3}{\partial \varphi^2}\right) = \frac{\mathrm{i}k}{n_1}(\eta^{-1}n_2^{\mathrm{S}}|E_3|^2 + 2n_2^{\mathrm{F}})E_3, \tag{12a}$$

$$\frac{\partial E_3'}{\partial z} - \frac{\mathrm{i}}{2k}\left(\frac{1}{r}\frac{\partial E_3'}{\partial r} + \frac{\partial^2 E_3'}{\partial r^2} + \frac{1}{r^2}\frac{\partial^2 E_3'}{\partial \varphi^2}\right) = \frac{\mathrm{i}k}{n_1}(\eta n_2^{\mathrm{S}'}|E_3'|^2 + 2n_2^{\mathrm{F}'})E_3', \quad (12b)$$

where $\eta = \omega_2^2/\omega_1^2$, which indicates that coupling interaction depends on the frequency ratio of two components. The $n_2^{\mathrm{S,S}'}$ are self-Kerr nonlinear coefficients of E_3 and E_3', $n_2^{\mathrm{F}} = n_2^{\mathrm{X1}}|E_1|^2 + n_2^{\mathrm{X2}}|E_1'|^2 + n_2^{\mathrm{X3}}|E_3'|^2$ and $n_2^{\mathrm{F}'} = n_2^{\mathrm{X1}'}|E_1|^2 + n_2^{\mathrm{X2}'}|E_1'|^2 + n_2^{\mathrm{X3}'}|E_3|^2$ are governed by XPM.

To understand the physics behind the existence of an interaction between two azimuthons, it is useful to discuss the phenomenon of a vortex-induced waveguide. For two probe fields E_3 and E_3' with similar powers, the linear waveguide approximation is invalid.[22] In the nonlinear waveguide region, the mutual incoherent coupling between two azimuthon beams gives rise to vector azimuthons. There exists a mutual attraction force in the self-defocusing region. Furthermore, the strong dressing field E_1' plays a very important role in the formation of vector azimuthons. The enhanced cross-Kerr nonlinear induced by E_1' could counterbalance the azimuthal instability and suppress the breakup of multi-component structure. Therefore, the stable three-spot vector azimuthons form in the self-defocusing region.

Now, we discuss the superposition of a stronger degenerate FWM signal E_{F1} and a weak nondegenerate signal E_{F3}. When E_1, E_1', E_3, and E_3' are turned on, a DFWM signal E_{F1} (with frequency ω_1) and an NDFWM signal E_{F3} (with frequency ω_2) are generated simultaneously and they co-propagate in the same direction. As discussed above, in a V-type three-level system, the DFWM signal E_{F1} can form three-spot azimuthon, while the NDFWM signal E_{F3} shows a dipole-shape structure. When E_{F1} is much greater than E_{F3}, the linear waveguide approximation is valid. The azimuthon beam E_{F1} induces an attractive potential, which is named a vortex-induced waveguide. The weak E_{F3} is trapped by this waveguide and propagates as a guided mode. Therefore, E_{F1} and E_{F3} fuse to form a new composite beam. However, this structure is unstable. It forms three-spot azimuthon only at appropriate frequency detuning, and decays into a rotating dipole-type shape with increasing Δ_1.

For comparison, figure 5(b) gives the multi-component azimuthons obtained in a two-level system. When four laser beams E_1, E_1', E_3, E_3' (or E_1, E_1', E_2, E_3') are turned on, the superposition $E_{\mathrm{F1+F3}}$ (or $E_{\mathrm{F1+F5}}$) is obtained. In a two-level system, both DFWM signal and NDFWM signals can form azimuthons. The mutual incoherent coupling between two azimuthon beams results in stable multi-component azimuthons in the self-defocusing region. When E_2, E_1', E_3, E_3' are turned on, we can obtain two NDFWM signals E_{F5} (ω_2) and E_{F5} ($2\omega_2 - \omega_1$) co-propagate in the same direction. We can see that the two azimuthon beams with similar powers also generate a stable double-azimuthon structure in the self-defocusing region. When six laser beams ($E_{1,2,3}$ and $E_{1,2,3}'$) are all turned on, one strong azimuthon beam E_{F1} and three weak vortex beams $E_{\mathrm{F3,F5,F6}}$ co-propagate in the opposite direction of $\boldsymbol{k}_1'$. The superposition of these four co-propagating azimuthons forms a four-component azimuthon beam. Compared with the V-type three-level system, it is beneficial to generate multi-component azimuthons in the two-level system.

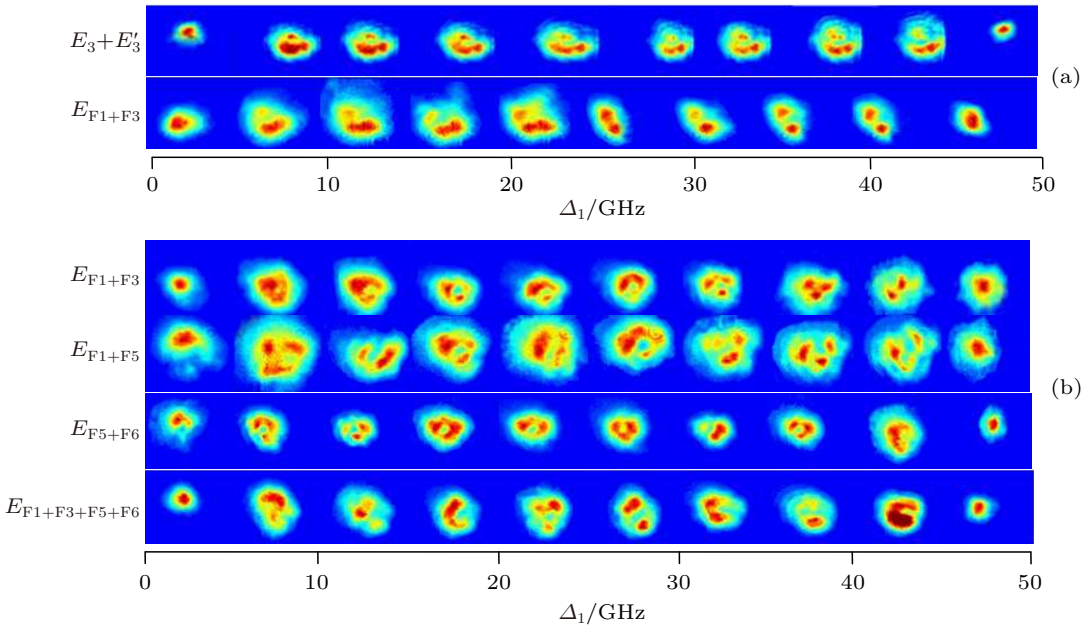


Fig. 5. Azimuthon spatial vector solitons in (a) V-type three-level system and (b) two-level system.

5. Conclusion

In conclusion, we have investigated, experimentally and theoretically, the formation of the multi-component optical azimuthons of FWM in V-type three-level and two-level systems. We have observed the transformations among vortex beams, three- or four-spot azimuthons, dipole and fundamental beams through XPM. We have also observed vector azimuthons and discuss the mutual incoherent coupling between two components. Moreover, we have compared the stabilities of azimuthons in V-type three-level and two-level atomic systems. It is more appropriate to generate stable azimuthons in a two-level system than in a V-type three-level system.

References

[1] Desyatnikov A S, Kivshar Y S and Torner L 2005 *Prog. Opt.* **47** 291

[2] He Y J, Malomed B A and Wang H Z 2007 *Opt. Express* **15** 17502

[3] Desyatnikov A S, Sukhorukov A A and Kivshar Y S 2005 *Phys. Rev. Lett.* **95** 203904

[4] Zhang Y, Skupin S, Maucher F, Pour A G, Lu K and Krolikowski W 2010 *Opt. Express* **18** 27846

[5] Li J, Wang D S, Wu Z Y, Yu Y M and Liu W M 2012 *Phys. Rev. A* **86** 023628

[6] Zhang Y P, Nie Z Q, Zhao Y, Li C B, Wang R M, Si J H and Xiao M 2010 *Opt. Express* **18** 10963

[7] Zhuang Y M, Sang S L, Li P Y, Yuan C Z, Huo S L, Xue X X, Wang Z G, Zheng H B and Zhang Y P 2012 *Chin. Phys. B* **21** 024204

[8] Wang R M, Wu Z K, Zhang Y Q, Zhang Z Y, Yuan C Z, Zheng H B, Li Y Y, Zhang J H and Zhang Y P 2012 *Opt. Express* **20** 14168

[9] Zhao Y, Nie Z Q, Zhang Y P, Gan C L, Zheng H B, Li Y Y and Lu K Q 2009 *Chin. Phys. B* **18** 2340

[10] Michinel H and Paz-Alonso M 2006 *Phys. Rev. Lett.* **96** 023903

[11] Skupin S, Saffman M and Krolikowski W 2007 *Phys. Rev. Lett.* **98** 263902

[12] Yang W X, Chen A X, Lee R K and Wu Y 2011 *Phys. Rev. A* **84** 013835

[13] Lederer F, Stegeman G I, Christodoulides D N, Assanto G, Segev M and Silberberg Y 2008 *Phys. Rep.* **463** 1

[14] Chen W C, Xie J N, Lu H and Xu W C 2003 *Chin. Phys. Lett.* **20** 1286

[15] Musslimani Z H, Soljacic M, Segev M and Christodoulides D N 2001 *Phys. Rev. E* **63** 066608

[16] Desyatnikov A S and Kivshar Y S 2001 *Phys. Rev. Lett.* **87** 033901

[17] Salgueiro J R and Kivshar Y S 2004 *Phys. Rev. E* **70** 056613

[18] Liu X M, Zhou X Q and Lu C 2005 *Phys. Rev. A* **72** 013811

[19] Liu X M 2008 *Phys. Rev. A* **77** 043818

[20] Masajada J and Dubik B 2001 *Opt. Commun.* **198** 21

[21] Liu J S, Hao Z H 2002 *Chin. Phys.* **11** 0254

[22] Carlsson A H, Malmberg J N, Anderson D, Lisak M, Ostrovskaya E A, Alexander T J and Kivshar Y S 2000 *Opt. Lett.* **25** 660